JCB Article

Characterization of Cep135, a novel coiled-coil centrosomal protein involved in microtubule organization in mammalian cells

Toshiro Ohta,[1] Russell Essner,[1] Jung-Hwa Ryu,[1] Robert E. Palazzo,[2] Yumi Uetake,[1] and Ryoko Kuriyama[1]

[1]Department of Genetics, Cell Biology, and Development, University of Minnesota, Minneapolis, MN 55455
[2]Department of Molecular Biosciences, University of Kansas, Lawrence, KS 66045

By using monoclonal antibodies raised against isolated clam centrosomes, we have identified a novel 135-kD centrosomal protein (Cep135), present in a wide range of organisms. Cep135 is located at the centrosome throughout the cell cycle, and localization is independent of the microtubule network. It distributes throughout the centrosomal area in association with the electron-dense material surrounding centrioles. Sequence analysis of cDNA isolated from CHO cells predicted a protein of 1,145–amino acid residues with extensive α-helical domains. Expression of a series of deletion constructs revealed the presence of three independent centrosome-targeting domains. Overexpression of Cep135 resulted in the accumulation of unique whorl-like particles in both the centrosome and the cytoplasm. Although their size, shape, and number varied according to the level of protein expression, these whorls were composed of parallel dense lines arranged in a 6-nm space. Altered levels of Cep135 by protein overexpression and/or suppression of endogenous Cep135 by RNA interference caused disorganization of interphase and mitotic spindle microtubules. Thus, Cep135 may play an important role in the centrosomal function of organizing microtubules in mammalian cells.

Introduction

The centrosome in animal cells is composed of a pair of centrioles and a surrounding amorphous cloud of pericentriolar material. It is responsible for the assembly of microtubules and the organization of higher-ordered, microtubule-containing structures. Because these microtubules are required for a number of vital cellular functions, it is important to identify and characterize the molecular components of the centrosome.

The centrosome and its associated proteins have been analyzed by multiple strategies, including genetic screens, generation and characterization of antibody probes, and protein biochemical analysis (for review see Andersen, 1999). Nonetheless, understanding the molecular composition of the centrosome is still far from complete. This is in part due to the fact that, unlike other microtubule organizing centers (MTOCs),* such as spindle pole bodies in yeast (Wigge et al., 1998; Francis and Davis, 2000), the pericentriolar material of the centrosome is featureless and tends to become fragmented during sample preparation. In addition, the centrosome is known to act as a cell center, attracting a number of other noncentrosomal molecules into and around it. This makes it difficult to distinguish components directly involved in centrosomal activities from those that are associated with the centrosomal structure in a nonspecific manner.

Because centrosomes/MTOCs direct the organization of highly dynamic microtubule arrays, they must contain specific components responsible for microtubule nucleation, orientation, and anchorage. It is now well established that individual microtubules are nucleated from 25-nm ring structures distributed throughout the pericentriolar material. Such rings, called γ-TuRCs, are composed of γ-tubulin plus six to seven additional minor components (for review see Wiese and Zheng, 1999). To anchor the minus end of microtubules, molecules with an affinity for the end and/or wall of microtubules, such as microtubule-associated proteins (MAPs) (Kellogg et al., 1989) and ninein (Mogensen et al., 2000), are embedded in the pericentriolar material. To

Address correspondence to Ryoko Kuriyama, Department of Genetics, Cell Biology, and Development, 6-160 Jackson Hall, 321 Church St. S.E., University of Minnesota, Minneapolis, MN 55455. Tel.: (612) 624-0471. Fax: (612) 626-6140. E-mail: ryoko@lenti.med.umn.edu

*Abbreviations used in this paper: GFP, green fluorescence protein; HA, hemagglutinin; MAP, microtubule-associated proteins; MTOC, microtubule organizing center; pBS, pBluescript; PBS-Tw20, Tween-20–containing PBS; siRNA, small interfering RNA; RNAi, RNA interference.

Key words: centrosome; pericentriolar material; mitotic spindle; coiled-coil protein; RNAi

The Journal of Cell Biology, Volume 156, Number 1, January 7, 2002 87–99
http://www.jcb.org/cgi/doi/10.1083/jcb.200108088

orientate microtubules, γ-TuRCs must be held together and connected to the pericentriolar material by attachment to structural elements (for reviews see Mazia, 1987; Kimble and Kuriyama, 1992). Recent studies on isolated centrosomes by fluorescence image-deconvolution microscopy has indicated that γ-tubulin exists as a unique lattice in association with pericentrin, a highly coiled-coil centrosomal protein (Dictenberg et al., 1998). The presence of a salt-insoluble, fibrous network capable of binding γ-tubulin has also been demonstrated in centrosomes isolated from clam (*Spisula)* oocytes (Schnackenberg et al., 1998). Because cells display a wide range of microtubule organizing patterns, it is reasonable to speculate that a number of structural components are located in the centrosome for arranging microtubule nucleating sites and maintaining the overall shape of the pericentriolar material. In fact, much evidence indicates that the majority of centrosome/MTOC proteins thus far characterized are structural proteins, like pericentrin, with predicted coiled-coil domains as a predominant structural feature (for reviews see Kimble and Kuriyama, 1992; Stearns and Winey, 1997).

Here we report the identification of a novel structural protein termed Cep135, a 135-kD centrosomal protein, in mammalian cells. It was originally identified by monoclonal antibodies raised against isolated centrosomes from *Spisula* oocytes (Vogel et al., 1997; Kuriyama et al., 2001). Cep135 is present in a wide range of organisms, indicating that it is a universal component of the centrosome. cDNA encoding the full-length Cep135 predicts a highly coiled-coil protein with three independent targeting domains. Overexpression of Cep135 polypeptides caused the formation of extraordinary fibrous polymers in both the centrosome and the cytoplasm. Altered levels of Cep135 concentration by protein overexpression and RNA interference (RNAi) profoundly affected the microtubule pattern in transfected cells. It is thus suggested that Cep135 may play an important role in organizing the functional centrosome.

Results

Identification of Cep135

By immunoscreening a CHO expression library with monoclonal anti–clam centrosome antibodies, we obtained a clone (A5–1-0) that included a 1.7-kb insert. Polyclonal antibodies raised against bacterial fusion proteins demonstrated that the antigen is present exclusively in the centrosomal region of both interphase (Fig. 1 A) and mitotic (Fig. 1 B) CHO cells. Double immunostaining with antibodies specific to known centrosomal components, such as pericentrin and γ-tubulin, provided evidence that the immunoreactive dots stained by the polyclonal antibody were indeed centrosomes (unpublished data). On immunoblots, the antibody recognized a single band with an apparent molecular mass of 135 kD that was present in whole cell lysates and copurified with isolated mitotic spindles (Fig. 1 C).

Cep135 localization at the centrosome is independent of the microtubule network. Fig. 2, A and B, illustrates cells treated with nocodazole to depolymerize microtubules. The protein remained at the centrosome (Fig. 2, A and B), which was identified by double staining with either anti–γ-tubulin (Fig. 2 B′) or pericentrin (unpublished data) antibodies. It was shown before that mouse embryonic fibroblasts lacking the p53 tumor suppressor protein induce multiple centrosomes (Fukasawa et al., 1996). The antigen colocalized at each dot with other centrosomal proteins (Fig. 2, C and C′). These results indicate that the protein encoded by A5–1-0 is an integral component of the centrosome, thus we named it a 135-kD centrosomal protein, Cep135.

Because Cep135 from CHO cells was originally identified by the antibodies raised against *Spisula* centrosome antigens, the protein is likely to be present in a wide range of organisms. Immunostaining as well as immunoblot analysis revealed that all mammalian cells tested so far (HeLa, PtK_1, $LLC\text{-}PK_1$, COS-7, 3T3, 293, mink lung epithelial cells, human and rat hepatocytes, Indian muntjac skin cells, and bovine lung endothelial cells) contained Cep135 and/or its homologues in the centrosome; the molecular mass of these homologues ranged from 120 to 140 kD (unpublished data). Positive immunostaining of the centrosome was also detected in nonmammalian cells. Fig. 2, D and E, shows the centrosomes in *Xenopus* cultured fibroblasts and dividing sea urchin eggs stained with mammalian anti-Cep135 antibodies. Cep135 may thus represent a universal component of centrosomes.

Immunolocalization of Cep135 in the centrosome

To further characterize the location of Cep135 within the centrosome, we performed immunoelectron microscopy. Fixed CHO cells were permeabilized with detergent and incubated with the polyclonal anti-Cep135 antibody that was

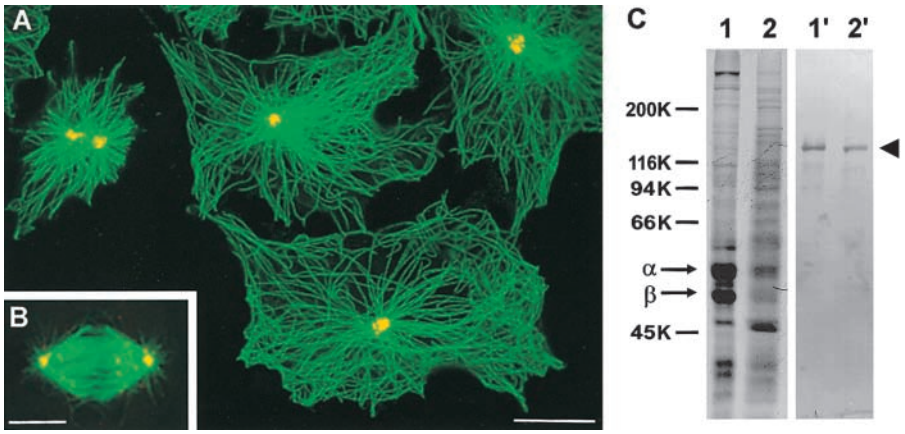

Figure 1. **Identification of Cep135 in the mammalian centrosome.** CHO cells at interphase (A) and mitosis (B) are double immunostained with anti-tubulin (green) and anti-Cep135 (yellow) antibodies. (C) Proteins prepared from isolated mitotic spindles (lanes 1 and 1′) and whole cell lysates (lanes 2 and 2′) were run on 7.5% SDS-PAGE and immunoblotted with polyclonal anti-Cep135 bacterial fusion protein antibodies (lanes 1′ and 2′). An arrowhead indicates the position of the 135-kD band recognized by the anti-Cep135 antibody. The positions of α- and β-tubulin are also indicated by arrows. Bars: (A) 10 μm; (B) 5 μm.

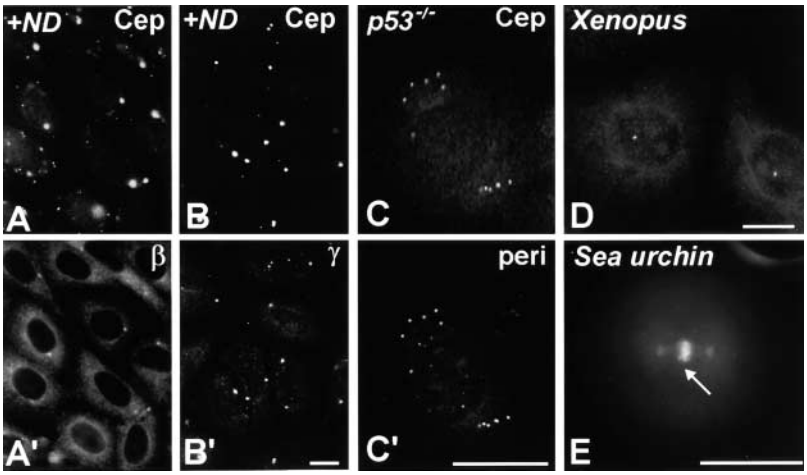

Figure 2. **Localization of Cep135 at the centrosome in nocodazole-treated CHO cells (A, A′, B, and B′), mouse embryonic fibroblasts lacking p53 (C and C′), frog fibroblasts (D), and sea urchin eggs (E).** Cells were double stained with anti-Cep135 (A–C) and either anti–β-tubulin (A′), anti–γ-tubulin (B′), or anti-pericentrin (C′) antibodies. Cep135 is present in the centrosome in a microtubule-independent manner. Interphase centrosomes and spindle poles in nonmammalian cells also contain the Cep135 antigen (D and E). An arrow indicates mitotic chromosomes aligned at the metaphase plate. Bars: (A–D) 10 μm; (E) 50 μm.

visualized by gold-conjugated secondary antibodies. In Fig. 3 A, two centrioles are seen at a juxtanuclear position. The Cep135 antigen is localized around the centrioles (arrowheads) and the electron-dense material surrounding the centrioles (arrows). In contrast, purified preimmune IgG showed no specific affinity to the centrioles or the pericentriolar material in control cells (unpublished data). Antigen distribution was also examined in mitotic spindles isolated from synchronized M phase cells. Fig. 3 B represents the polar region of an isolated spindle with microtubules emanat-

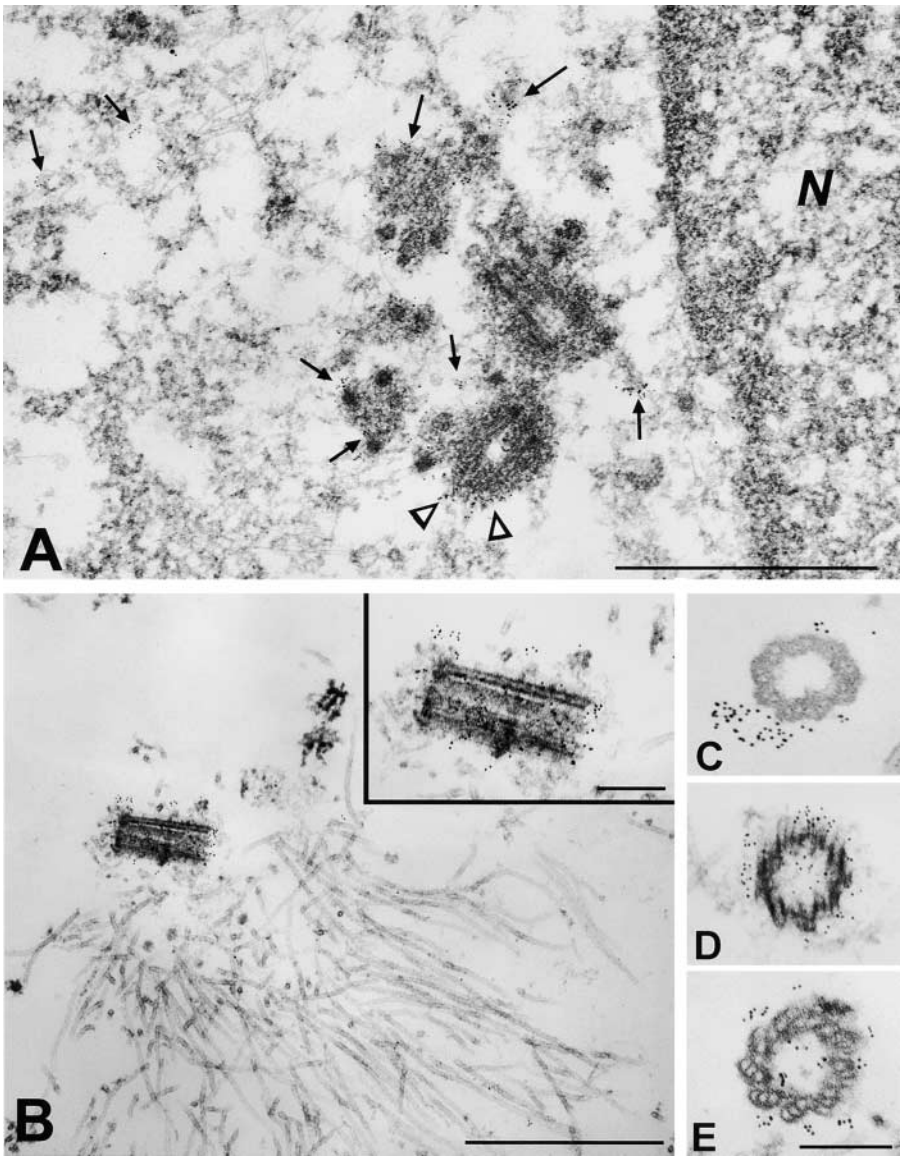

Figure 3. **Immunoelectron microscopy of Cep135 in interphase CHO cells (A) and isolated mitotic spindles (B).** 6-nm gold-conjugated Cep135 antibodies were detected around the centrioles (arrowheads) and in the amorphous material (arrows) in the centrosome located next to the nucleus (N). At the pole, in isolated mitotic spindles, Cep135 is present in close association with the centriole, both outside (C) and inside (D and E) the centriole wall. Bars: (A and B) 1 μm; (C–E) 0.2 μm.

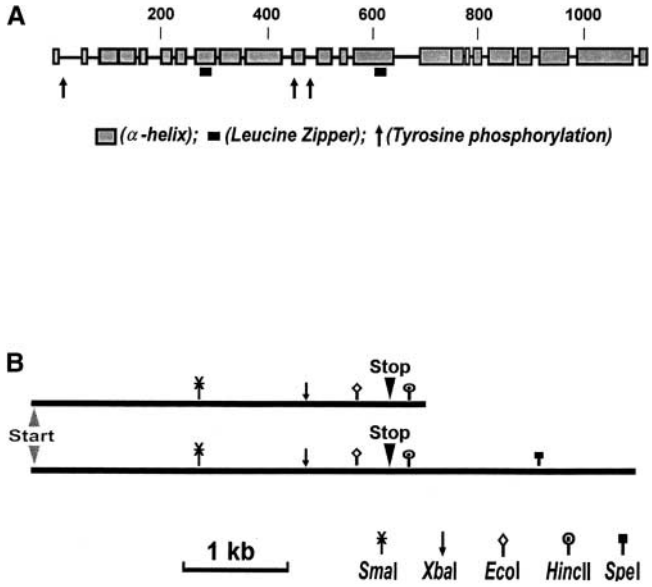

Figure 4. **Schematic diagram of the secondary structure of Cep135 (A) and the presence of two types of Cep135 transcripts in CHO cells (B).** (A) The protein consists of 1,145-amino acid residues in which extensive α-helical domains (shaded blocks) span almost the continuous length of polypeptide chain. The positions of two leucine zipper consensus motifs and three putative tyrosine phosphorylation motifs are indicated by black boxes and arrows, respectively. Numbers indicate the position of amino acids. (B) 10 cDNA clones isolated by screening of a CHO expression library are classified into two categories. All clones share the overlapping restriction maps and identical Cep135 coding sequence. Indicated are the start and stop codons as well as some restriction sites included in the sequences.

ing from the pole. The centrosomes of isolated spindles generally contain less amounts of the electron-dense cloud than in whole cells, and gold particles are detected in close association with the centriole (inset). Interestingly, staining was observed both outside (Fig. 3 C) and inside the microtubular wall of the centriole (Fig. 3, D and E). Both light and electron microscopy revealed that Cep135 is always confined to a smaller area in mitotic cells than in interphase cells. These results suggest that Cep135 is tightly attached to the centrosome at the spindle pole.

Isolation and characterization of cDNA encoding Cep135

cDNA clones encoding the full sequence of Cep135 were isolated by combining cDNA library screening and 5′-RACE protocols (the complete sequence was deposited in the GenBank/EMBL/DDBJ databank). The longest open reading frame predicts a protein of 1,145 amino acids with a calculated molecular mass of 134 kD. Sequence analysis indicates the presence of extensive α-helical coiled-coil domains spanning almost continuously the length of the protein (Fig. 4 A). It also includes two repeats with a hypothetical leucine zipper motif at amino acid positions 273–292 and 608–626 (Fig. 4 A, black boxes), implying that Cep135 is involved in protein–protein interaction. In addition, three putative tyrosine phosphorylation consensus motifs were identified (arrows), suggesting the possibility that Cep135 is a phosphoprotein.

On the basis of our sequence for Cep135, a human homologue(s) of Cep135 was identified in the expressed sequence tag databank. We also identified an additional clone (KIAA0635) isolated from a size-fractionated human brain cDNA library (Ishikawa et al., 1998). This clone overlaps with CHO Cep135 at amino acid positions 295–1141 (80% identity). The deduced amino acid sequence of CHO Cep135 shares no significant homology with any other known molecules. However, based on the ProSearch analysis designed to find the putative protein family (Hobohm and Sander, 1995), there is a >87 and >80% chance that Cep135 is in the same family with Spc110p/Nuf1p and Zip1, respectively. Like Cep135, a yeast spindle pole body component of Spc110p/Nuf1p (Kilmartin et al., 1993) and a synaptonemal complex protein of Zip1 (Sym and Roeder, 1995) are speculated to be highly coiled-coil proteins.

By rescreening the CHO library with the original Cep135 clone (A5–1-0), we obtained 10 additional cDNA fragments coding for different parts of the Cep135 sequence. All clones contain a poly(A)$^+$ stretch and share overlapping restriction maps. Nucleotide sequence analysis allowed for the classification of these cDNA clones into two categories (Fig. 4 B), which likely correspond to two transcripts (4.0 and 6.5 kb) detected by Northern blot analysis (unpublished data). Although the two coding sequences are identical, clones containing the longer insert have a ~2.5-kb 3′-untranslational sequence. Diversity within each category of clones was also noted in the nucleotide sequence of the 3′-untranslational region where there were obvious deletions just upstream of the poly(A)$^+$ tails (unpublished data).

Expression of Cep135 polypeptides in CHO cells

To identify subregions of Cep135 involved in centrosomal targeting, we prepared a series of deletion constructs, and expressed truncated polypeptides in CHO cells by transient transfection. As summarized in Fig. 5, construct #10 corresponds to the nearly full-length sequence lacking 28 amino acids at the NH_2 terminus. NH_2-terminal 15, 28, and 70% sequences were included in Δ1, Δ2, and Δ3 constructs, respectively. Constructs #0 (the original clone iso-

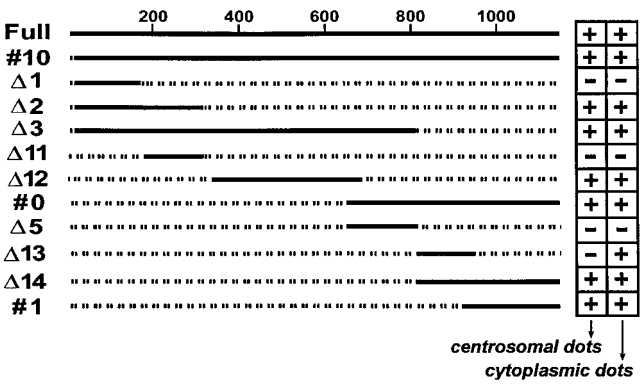

Figure 5. **A map of deletion constructs created for identification of the centrosomal target domain in Cep135.** Numbers indicate the positions of amino acids. The results of the immunolocalization of HA-tagged polypeptides at the centrosome and in the cytoplasm are summarized at the right.

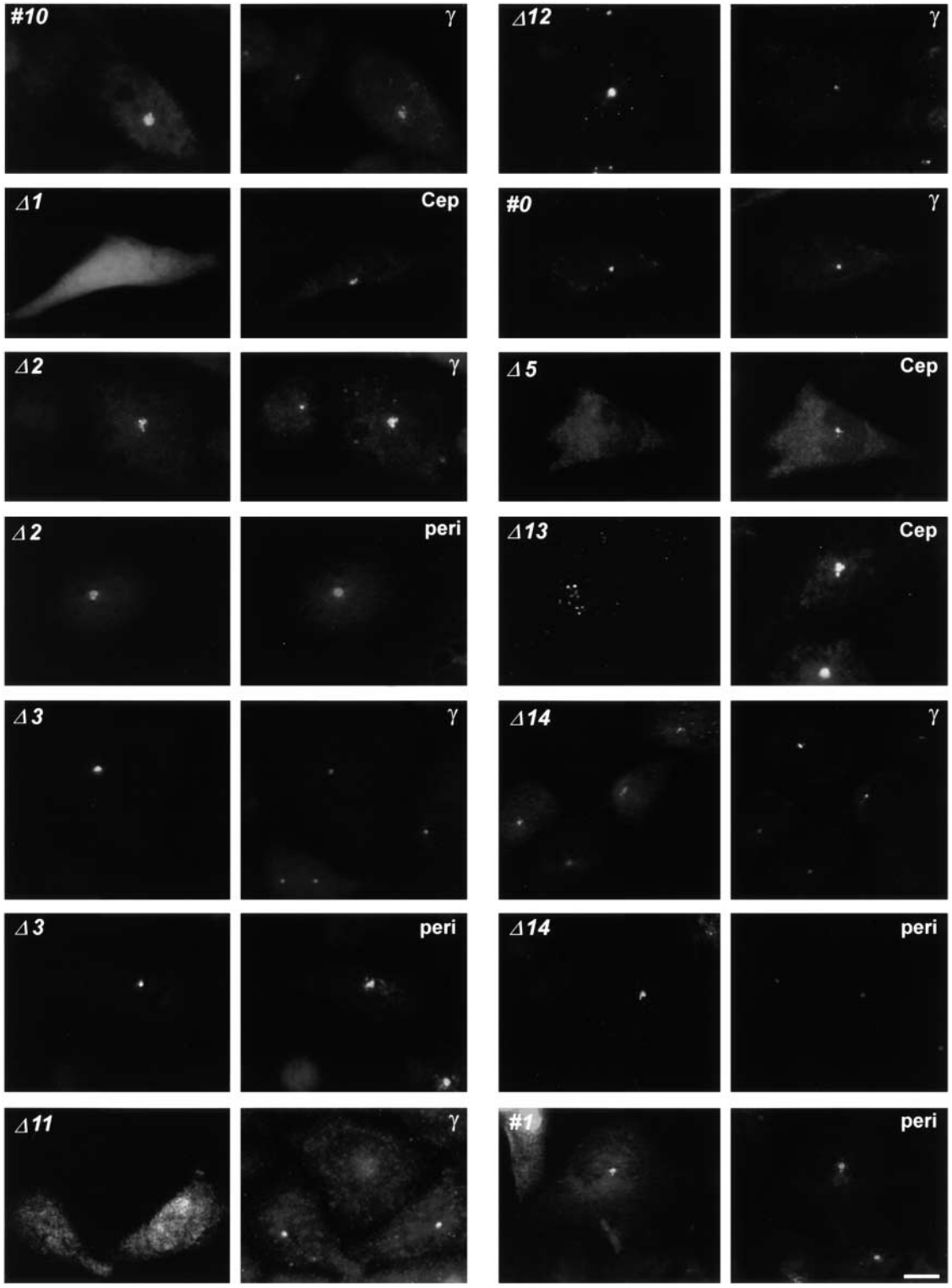

Figure 6. **Immunolocalization of truncated Cep135 polypeptides expressed in CHO cells by transient transfection.** The same cells are seen by double immunostaining with anti-HA (left side of each pair) and with either anti–γ-tubulin, anti-Cep135, or anti-pericentrin antibodies as indicated in each frame. Although the sequences encoded by Δ1, Δ11, Δ5, and Δ13 are not found in the centrosome, other clones produce proteins recruited to the centrosome. Note the NH_2-terminal Δ1 and Δ11 proteins in the cytoplasm are not recognized by the Cep135 antibody raised against the COOH-terminal #0 sequence. Bar, 10 μm.

lated from the library screening), Δ5, Δ13, Δ14, and #1 cover the COOH-terminal coding sequence. After confirming the expression of all of these truncated polypeptides on immunoblots (unpublished data), the subcellular distribution of tagged molecules was examined by fluorescence microscopy (Fig. 6). Exogenous proteins derived from clones #10, Δ2, Δ3, and Δ12 became visible as a dot(s) colocalized with other centrosomal components, in-

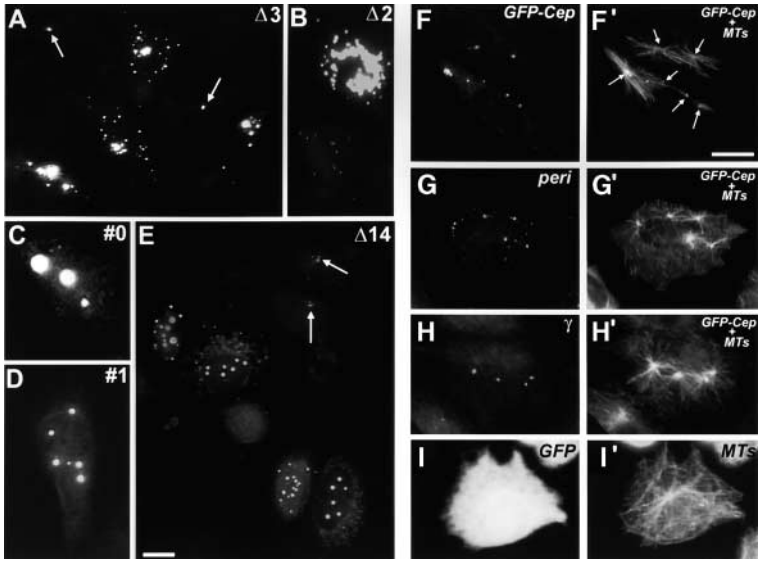

Figure 7. **Overexpression of Cep135 polypeptides causes the formation of cytoplasmic foci.** (A–E) Dots of various size and number were detected in cells overexpresssing different domains of the Cep135 sequence. The foci containing the COOH-terminal domain of Cep135 (#0, #1, and Δ14) show smooth and well-rounded surfaces. Arrows indicate the position of HA-tagged Δ3 and Δ14 that were successfully targeted to the centrosome as determined by γ-tubulin staining. (F–I′) Cytoplasmic dots containing the full-coding sequence of GFP-labeled Cep135 nucleate microtubules in vivo upon release from nocodazole treatment. Cells expressing GFP–Cep135 were treated with nocodazole for 2 h to depolymerize in situ microtubules. 5–15 min after removing nocodazole, cells were fixed, stained with anti-β-tubulin antibodies, and visualized for GFP–Cep135 (F′, G′, and H′). In addition to Cep135 (F), the dots are associated with pericentrin (G) and γ-tubulin (H). I and I′ show the control cell expressing a GFP leader sequence only. Bars, 10 μm.

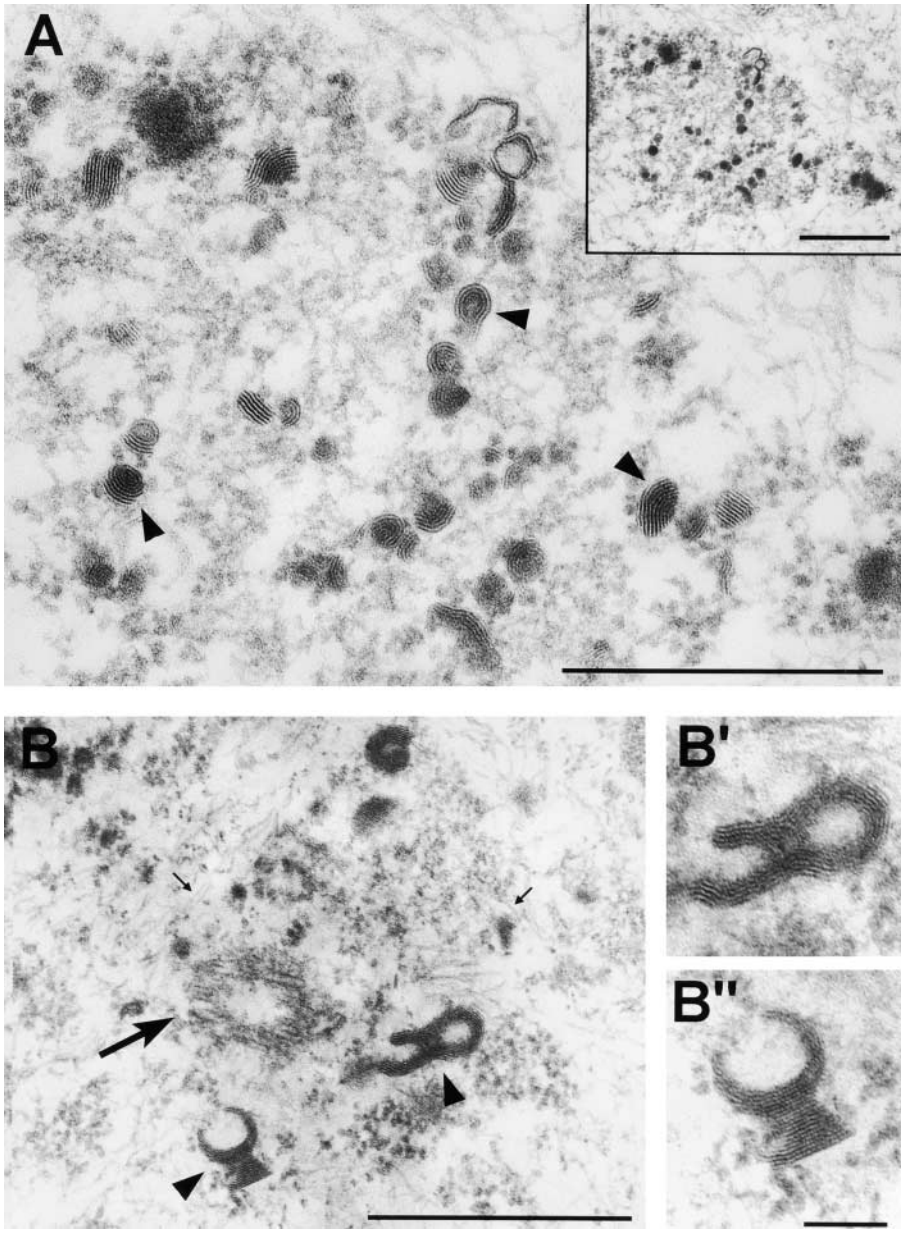

Figure 8. **Induction of fibrous aggregates in the centrosome (A and B) and the cytoplasm (C and D).** (A) A cell expressing GFP-tagged Δ3 includes a centrosome that appears as a large electron-dense cloud (oval area within inset at lower magnification) containing characteristic whorl-like particles (A, arrowheads). (B) Similar whorl-like particles of various shapes and sizes (arrowheads; B′ and B″ at higher magnification) and 6-nm fibers (small arrows) are seen in the centriole (large arrow)-containing centrosome. (C and D) The cytoplasmic dots are composed of electron-dense, curved aggregates. Similar to the whorls seen in A and B, the filamentous aggregates are composed of dense, curved parallel lines arranged with a periodicity of 6 nm. Bars: (A and B) 0.5 μm; (B′ and B″) 0.1 μm; (C and D) 0.5 μm.

cluding γ-tubulin (#10, Δ2, Δ3, Δ12) and pericentrin (Δ2 and Δ3). In contrast, the protein encoded by clones Δ1 and Δ11 was diffusely distributed in the cytoplasm. On the COOH-terminal side, clones #0, Δ14, and #1 induced proteins that were successfully recruited to the centrosome, identified by staining with either anti-Cep135 (Δ13), anti-γ-tubulin (#0 and Δ14), or anti-pericentrin (Δ14 and #1) antibodies. However, transfection of cells with plasmids containing Δ5 and Δ13 sequences failed to yield any positive centrosomal immunostaining. Because clones Δ2, Δ12, and #1 do not overlap (Fig. 5), it is reasonable to conclude that Cep135 contains at least three independent centrosomal target domains encoded by these clones. These domains span almost the entire length of the Cep135 sequence (Fig. 5).

Depending upon the level of protein expression, exogenous Cep135 resulted in the formation of immunofluorescence dots outside the centrosome. In Fig. 7, A and E, arrows indicate the centrosome to which hemagglutinin (HA)-tagged Δ3 and Δ14 were recruited. However, other cells in the same fields exhibit prominent Cep135-containing dots throughout the cytoplasm. Expression of all clones except Δ1, Δ11, and Δ5 produced such cytoplasmic dots of various sizes and numbers. Although the majority of dots are irregular in shape, foci composed of the COOH-terminal domains of the Cep135 sequence (#0, #1, and Δ14) contained smooth and well-rounded surfaces (Fig. 7, C–E). Some, but not all, dots were capable of acting as ectopic centrosomes/MTOCs. Fig. 7, F–I′ illustrates cells expressing green fluorescence protein (GFP)–tagged full-length polypeptides. Multiple dots induced in cells with GFP-tagged Cep135 (Fig. 7 F′, arrows), but not GFP alone (Fig. 7 I), were capable of organizing microtubules into astral arrays after release from nocodazole treatment. These dots were associated with not only Cep135 (Fig. 7, F and F′) but also pericentrin (G and G′) and γ-tubulin (H and H′).

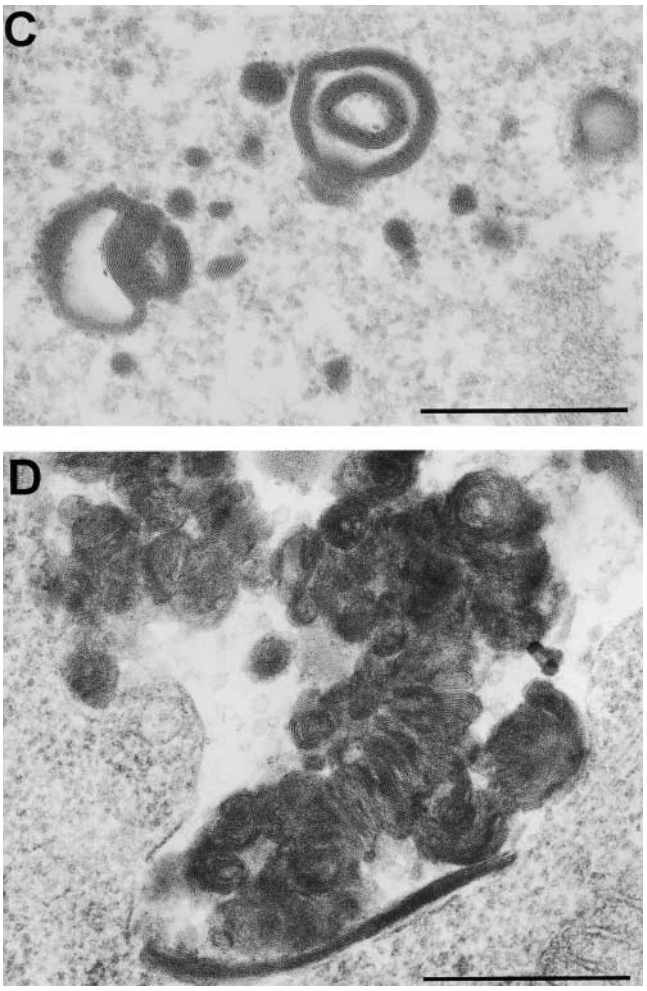

Figure 8 (continued)

Formation of fibrous aggregates in the centrosome and cytoplasm

Fig. 8, A and B, shows centrosomes included in the cells expressing the GFP-tagged Δ3 protein seen by thin section electron microscopy. The centrosomes appear as a distinctive electron-dense cloud, which is readily recognized at low magnifications (Fig. 8 A, inset). The centriole is visible in the plane of the section shown in Fig. 8 B (large arrow), whereas, in Fig. 8 A, no centrioles are visible. However, an abundance of 6-nm fibers (Fig. 8 B, small arrows) and electron-dense whorl-like structures (Fig. 8, A and B, arrowhead) were consistently observed in the pericentriolar material. The whorls are generally round in shape and are composed of repeating stacks of dark and light stripes organized in parallel curvilinear arrays with a periodic spacing of 6 nm. Identical whorl structures were also induced in cells expressing the GFP-tagged #10 polypeptide (unpublished data).

Overexpression of Cep135 proteins resulted in the formation of extra dots in the cytoplasm (Fig. 7). By electron microscopy, those dots were also seen to consist of repeating units identical to those in the whorls (Fig. 8, C and D). Although some of these cytoplasmic whorls have a similar appearance to those seen in the centrosome (Fig. 8 C), others appear as extensive masses of aggregated whorls (Fig. 8 D). The banding pattern in the whorls was not affected by treatment with detergents, suggesting that these structures are not membranous.

Effects of altered levels of Cep135 concentration on microtubule arrangement

Overexpression of Cep135. Expression of exogenous Cep-135 appears to be toxic given that considerably fewer mitotic cells were detected in GFP/HA fluorescence than in control cells. Therefore, in order to quantitatively analyze the mitotic profile, we synchronized cells and enriched mitotic cell populations. As summarized in Fig. 9, nearly 80% of transfected M phase cells contained spindles in abnormal shapes composed of severely disorganized microtubules and microtubule bundles (Fig. 9, A–C). These cells frequently contained fluorescent dots in various numbers and sizes. Whereas some dots were intensely stained with anti-tubulin antibodies (Fig. 9 D), others were attached to one end of disorganized microtubule bundles (Fig. 9, E and F).

RNAi directed against endogenous Cep135 in CHO cells. The role of Cep135 in microtubule organization was further analyzed by suppressing expression of the Cep135-

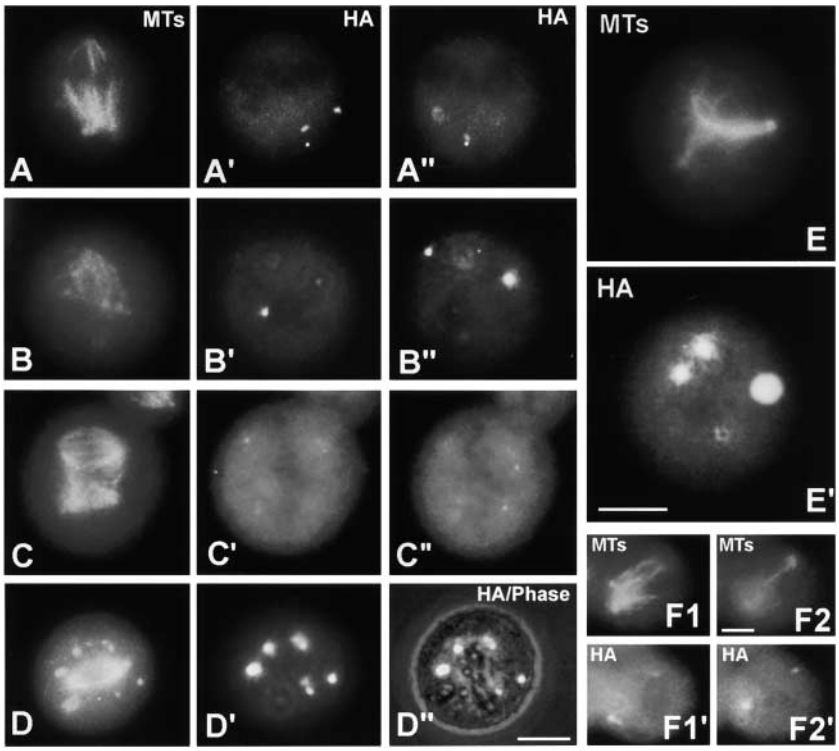

	Cells Expressing Cep135		Cells *NOT* Expressing Cep135	
spindles	normal	abnormal	normal	abnormal
Exp. I	9	58 (87%)	89	27 (23%)
Exp. II	15	57 (79%)	171	34 (17%)

Figure 9. **Abnormal mitotic spindles induced in cells overexpressing HA-tagged Δ3 polypeptides of Cep135.** The same cells are seen by fluorescence microscopy after double immunostaining with anti-tubulin and anti-HA antibodies as indicated in each figure. A′–C″ and F1–F2′ represent the images at different focal planes. D″ shows a double image of phase-contrast and fluorescence microscopy. Exogenous Δ3 Cep135 causes the formation of extra dots to which spindle microtubules are frequently attached (C, E, and F). Some dots are also labeled by anti–β-tubulin staining (D). Quantitative analysis of normal and abnormal spindles is summarized in the table. Note that the nocodazole treatment necessary to synchronize M phase cells resulted in the production of more abnormal cells (17–23%) than nontreated controls, which generally include less than 2–5% abnormal cells (Matuliene et al., 1999). Bar, 10 μm.

specific gene in CHO cells. Using the protocol recently established by Elbashir et al. (2001), we synthesized the 21–nucleotide small interfering RNA (siRNA) duplex to block Cep135-specific mRNA via RNAi. Immunoblot analysis showed that the level of endogenous Cep135 was reduced by ~50 and ~30% in cells fixed at 28 and 48 h after siRNA transfection (Fig. 10 A, RNAi-I). When the cells were further treated with additional siRNA, we detected only 10–15% Cep135 fluorescence remaining at the centrosome (Fig. 10 A, RNAi-II).

Cep135 gene expression silencing was further confirmed by immunofluorescence staining. Transfected cells (RNAi-I) showed dramatic reduction of Cep135 fluorescence at the centrosome (Fig. 10 B, b), which was in striking contrast with the control cells (Fig. 10 B, a). However, a single siRNA transfection appears to be insufficient to suppress Cep135 expression in all cells, as colonies of nontransfected cells became apparent after several days (arrowheads in Fig. 10 B, b). By repeating one (RNAi-II) or two (RNAi-III) more transfection steps, we were able to reduce the level of endogenous Cep135 in the vast majority of cells (Fig. 10 B, c and d). It is worthy to mention that Cep135 appears to be essential for cell viability because cell growth was hardly detected in siRNA-treated cells. Measurement of fluorescence intensity showed that the amount of endogenous Cep135 decreased to 40 (RNAi-I), 20 (RNAi-II), and 9% (RNAi-III) by RNAi. Frequency histograms summarized in Fig. 10 C indicate that the majority of transfected cells (RNAi-I, 66%; RNAi-II, 85%; and RNAi-III, 92%) expressed Cep135, and its fluorescence intensity was <25% of the average fluorescence in the mock cells.

To examine the effect of RNAi on microtubule organization, we double stained cells with α-tubulin and Cep-135 antibodies (Fig. 11). Although microtubule formation was relatively unaffected, over 50% of cells (RNAi-III) formed disorganized, unfocused microtubule arrays (Fig. 11 B′). A number of round cells detached and were floating in the culture medium during M phase. Immunostaining of harvested round cells revealed the presence of abnormal mitotic spindles: whereas some were in a multipolar configuration (Fig. 11 C′), others showed totally disorganized microtubule arrangement (Fig. 11 E′). Monopolar spindles were also frequently seen in cells (Fig. 11, C′ and D′) where chromosomes tended to be pushed away on one side (Fig. 11 D″). In Fig. 11, F–F″, the fluorescence signal of Cep135 was still detectable. Chromosome separation occurred normally but microtubules at the central spindle were quite disorganized (Fig. 11 F′). Those cells hardly completed cytoplasmic division, suggesting that Cep135 is important for the organization of functional mitotic spindles and completion of cytokinesis.

Discussion

We have described the identification of a novel centrosome protein, Cep135, that is present in a wide range of metazoan organisms. It is unique, but the ProSearch analysis (Hobohm and Sander, 1995) suggests that Cep135 might be in the same family as Spc110p/Nuf1p, a coiled-coil protein in the spindle pole body of yeast (Kilmartin et al., 1993). Because Tassin et al. (1998) have studied a 100-kD mammalian protein that cross-reacts with an antibody specific to yeast Spc110p, Cep135 might represent a novel protein that is not a mammalian homologue of Spc110p.

A number of centrosomal components thus far characterized, including Cep135, are rich in α-helix and coiled-coil (Kimble and Kuriyama, 1992; Stearns and Winey, 1997). Some of these domains may be related to those in intermedi-

ate filament proteins, as indicated by the fact that antibodies raised against MTOC/centrosome-containing fractions frequently cross react with intermediate filaments (for example see Buendia et al., 1990; Sellitto et al., 1992). Similarly, antibodies specific for different intermediate-like filament proteins (Schatten et al., 1987; Paul and Quarani, 1993) occasionally immunostain the centrosome and spindle poles. However, we did not detect any antibody cross-reactivity between Cep135 and intermediate filament structures or intermediate filament–like proteins.

Judging from the intracellular distribution of truncated polypeptides, we concluded that Cep135 contains at least three independent centrosome-targeting domains encoded by Δ2, Δ12, and #1 clones (Fig. 5). Centrosome localization domains have also been identified in *Drosophila* CP190 (Oegema et al., 1995). Because none of the Cep135 subdomains share sequence similarities with the centrosomal targeting sequence of CP190, identification of a consensus "centrosome localization signal," if any, must await further investigation. The mechanism by which Cep135 becomes associated with the centrosome is unknown. Preliminary results suggest that Cep135 in *Xenopus* egg extracts exists as a large protein complex (unpublished data). This may suggest that Cep135 becomes localized at the centrosome as a part of the multiprotein complex. All Cep135 subfragments that can be translocated to the centrosome contain extensive α-helices, and the hypothetical leucine zipper motif is included in the middle and NH_2-terminal domains (Fig. 4 A). These results suggest that recruitment of the protein to the centrosome is achieved through interactions with other coiled-coil proteins in the centrosome. Further biochemical analysis of Cep135 and the Cep135-containing fractions should elucidate the mechanism for targeting Cep135 to the centrosome.

Overexpression of Cep135 polypeptides resulted in the assembly of several unique structures in both centrosomes and the cytoplasm. First, the centrosome became associated with an abundance of 6-nm filaments and extraordinary whorl-like particles; the latter do not resemble the filamentous polymers produced by overexpression of other centrosome-related molecules, such as NuMA (Saredi et al., 1996). Because the whorls are composed of curvilinear dense lines with a regular 6-nm periodicity, it is conceivable that the whorls might be composed of 6-nm filaments aligned side by side and end to end. Three-dimensional aggregates of Cep135 may thus be distinct from paracrystals induced by overexpression of other coiled-coil proteins, including the myosin tail (Atkinson and Stewart, 1991), tropomyosin (Xie et al., 1994), intermediate filament proteins (Stewart et al., 1989), and nuclear lamins (Heitlinger et al., 1991). With higher levels of protein expression, more whorls of larger sizes were produced in the cytoplasm. It is possible that Cep135 filaments and whorls first emerge in the centrosomal region; the whorls may then appear outside the centrosome where their size gradually increases as the amount of protein increases. This could happen if the centrosome has a limited capacity to accommodate Cep135. Alternatively, excess amounts of Cep135 polypeptides may cause the immediate formation of massive filamentous aggregates before targeting to the centrosome.

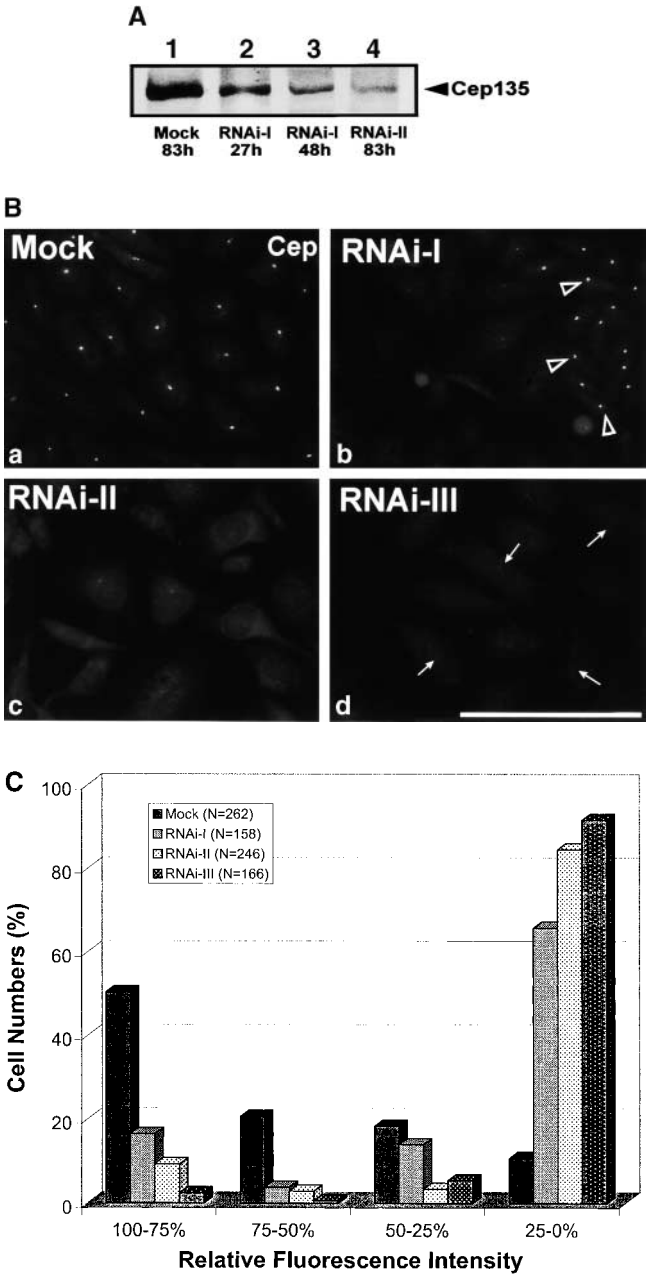

Figure 10. **Suppression of Cep135 expression by RNAi.** (A) Immunoblotting analysis: equal amounts of proteins prepared from CHO cells at 27 (lane 2), 48 (lane 3), and 83 h (lanes 1 and 4) after mock (lane 1), single (RNAi-I; lanes 2 and 3), and double (RNAi-II; lane 4) siRNA transfections were run on a 7.5% protein gel. Arrow indicates the position of Cep135 bands. (B) Immunofluorescence staining: mock- (a) and siRNA-treated (b–d) CHO cells were fixed at 72 (b and c) and 96 h (a and d) after transfection, and immunostained with Cep135; single (RNAi-I; b), double (RNAi-II; c), and triple (RNAi-III; d) RNAi. To correctly represent the amount of endogenous Cep135 in all cells, both mock- and siRNA-transfected cells were fixed and immunostained in an identical manner, and all images were captured and printed under identical conditions. Nontransfected cells in RNAi-I formed a colony as indicated by arrowheads (b), and arrows in RNAi-III indicate the position of weakly stained centrosomes (d). Bar, 50 μm. (C) Frequency histogram of Cep135 immunofluorescence intensity at the centrosome in mock- (Mock) and siRNA-transfected cells (RNAi-I, -II, and -III). Cells were classified into four categories: 100–75, 75–50, 50–25, and 25–0% of the Cep135 fluorescence intensity at the centrosome relative to the mean value of the centrosomal Cep135 fluorescence mock cells.

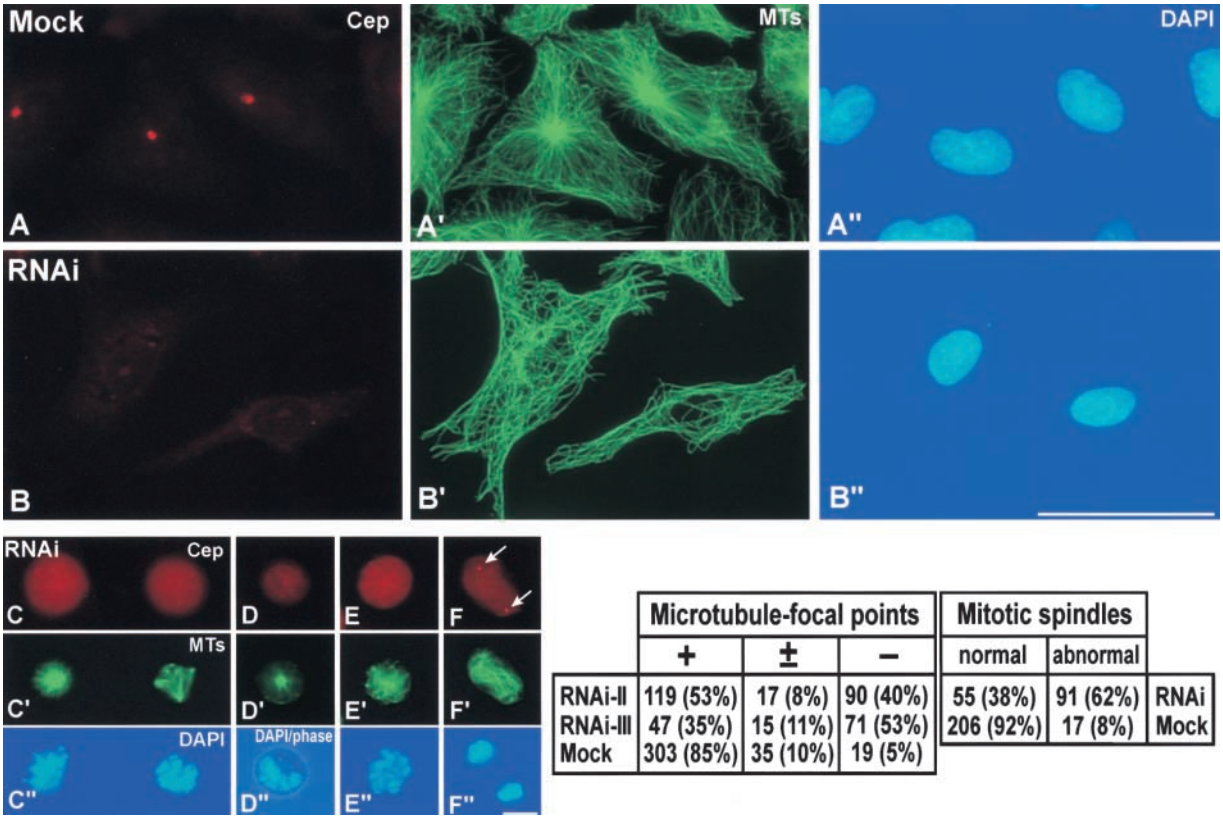

	Microtubule-focal points			Mitotic spindles		
	+	±	−	normal	abnormal	
RNAi-II	119 (53%)	17 (8%)	90 (40%)	55 (38%)	91 (62%)	RNAi
RNAi-III	47 (35%)	15 (11%)	71 (53%)	206 (92%)	17 (8%)	Mock
Mock	303 (85%)	35 (10%)	19 (5%)			

Figure 11. **RNAi causes abnormal organization of interphase and mitotic microtubules in CHO cells.** The same cells were stained with anti-Cep135 (A–F), anti–α-tubulin (A′–F′) antibodies, and DAPI (A″–F″). D″ shows a double image of phase-contrast and fluorescence microscopy. siRNA-transfected cells tended to lose the microtubule focal point during interphase (B′). Abnormal spindles in monopolar (C–C″ and E–E″) and multipolar (C–C″ and D–D″) orientation were frequently seen in mitotic cells. (F–F″) Cep135 was still weakly detected at each pole (arrows), but central spindle microtubules were severely disorganized. Tables summarize normal and abnormal microtubule patterns scored in interphase (RNAi-II and RNAi-III) and mitotic (RNAi-I + RNAi-II) cells. Bars: (A–B″) 50 μm; (C–F″) 10 μm.

Neither overexpression of full/truncated Cep135 polypeptides nor suppression of endogenous Cep135 by RNAi resulted in the inhibition of microtubule formation in vivo (Figs. 7 [F–I′], 9, and 11). Cep135 is not a member of the γ-TuRC complex (unpublished data), thus the protein could not be directly involved in the microtubule nucleating activity of the centrosome. Some dots, but not all, were attached to microtubules and capable of initiating microtubule polymerization in transfected cells (Figs. 7, F–I′, and 9). However, only subsets of Cep135-containing dots could form extopic centrosomes. This may imply that Cep135-containing dots are different from other ectopic centrosomes induced in cells overexpressing γ-tubulin (Shu and Joshi, 1995), aurora 2 kinase (Zhou et al., 1998), and Ran BMP (Nakamura et al., 1998) and in terms of the macromolecular composition as well as microtubule-nucleating activity. Although it may not be directly involved in microtubule nucleation onto the centrosome, Cep135 affects the overall pattern of microtubule distribution in interphase and mitotic cells. It is thus likely that Cep135 may be important for anchoring molecules essential for the establishment of the centrosome as an MTOC and/or a regulator of cellular activities (Doxsey, 2001).

We can speculate other possibilities regarding the function of Cep135 in the centrosome. Based on its molecular structure and capability to form extraordinary fibrous aggregates, the protein may be primarily responsible for proper organization and maintenance of the overall structure of the pericentriolar material. Indeed the centrosomes of transfected cells appear as prominent electron-dense masses, which are more easily recognized than in control cells (Fig. 8, A and B). We also noted an alteration in centrosome–nucleus interaction in transfected cells. In contrast to control cells, in which the centrosome and nucleus are adjacent and isolated as a unit complex upon cell lysis (Bornens, 1977; Kuriyama and Borisy, 1981), the cells with overexpressed Cep135 tend to release the centrosome from the otherwise tight nuclear association (unpublished data). The presence of excess Cep135 may increase the structural stability of the pericentriolar material, allowing the centrosome to maintain its integrity even under the severe conditions necessary to release the nucleus from a cell. In the relatively featureless pericentriolar material, Cep135 does not appear to show any preferential localization, unlike other centrosomal molecules, such as C-Nap1 (Fry et al., 1998), cenexin (Lange and Gull, 1995), centrin (Paoletti et al., 1996), Spc110/Nuf1p (Tassin et al., 1998), AKAP350 (Schmidt et al., 1999), and Odf2 (Nakagawa et al., 2001). The presence of Cep135 in an extended area of the centrosome favors our prediction that it

is a scaffolding protein important for maintaining the overall shape of the pericentriolar material in the centrosome.

The molecular structure of Cep135 is close to that of Spc110p/Nuf1p and Zip1, which are believed to serve as spacer proteins in the yeast spindle pole body (Kilmartin et al., 1993) and synaptonemal complex (Sym and Roeder, 1995). We have previously shown that baculovirus expression of Cep135 polypeptides causes the formation of higher-ordered polymers in insect Sf9 cells where they display a characteristic cross-striation pattern different from the whorls described here (Ryu et al., 2000). Of particular interest is the observation that the spacing changes according to the length of the Cep135 polypeptide: the longer the polypeptide length, the wider the space between two adjacent, dense bands. It will thus be interesting to examine whether Cep135, like Spc110and Zip1, functions as a ruler in the pericentriolar material.

The introduction of siRNA was remarkably effective in suppressing endogenous Cep135 levels in mammalian cells (Fig. 10). Further analysis of RNAi phenotypes would be useful for evaluating the mechanism of Cep135 function in the centrosome.

Materials and methods

Preparation of anticentrosome antibodies

Monoclonal anti–clam centrosome antibodies were prepared as described previously (Kuriyama et al., 2001). In brief, the centrosomal fraction was purified from oocytes of the surf clam, *Spisula solidissima*, by differential centrifugation and sucrose density gradient centrifugation (Vogel et al., 1997). The native and denatured centrosomal proteins were added to SDS sample buffer and injected into mice intravenously at 2–3 week intervals. Immunized spleens were fused with myeloma cells (American Type Culture Collection; accession number P3X63-AG8.653) to generate monoclonal antibodies (Kuriyama and Ensrud, 1999). After screening hybridoma supernatants by indirect immunofluorescence staining of isolated clam centrosomes, positive clones were further subcloned two to three times by limiting dilutions. Determination of immunoglobulin species and preparation of ascites fluid were performed according to the procedures outlined before (Kuriyama and Ensrud, 1999).

Polyclonal Cep135 antibodies were raised against #0 and #10 coding sequences (see below) in both rabbits and mice. Proteins fused with glutathione *S*-transferase were expressed in bacteria as outlined previously (Kuriyama et al., 1995).

Cloning of mammalian Cep135 cDNA and construction of expression vectors

A commercially available CHO cell cDNA expression library cloned in λUni-Zap (Stratagene) was immunoscreened with the mixture of monoclonal antibodies prepared as outlined above. One positive clone (A5–1-0) was isolated and its 1.7-kb insert was excised and used as a probe for further screening of the same library. This screening yielded ten additional clones (A5–1-1 to A5–1-10) with insert sizes ranging from 1.9 to 4.6 kb (Fig. 4 B). The 5′ sequence containing the start codon was extended from clone #10 using a commercially available 5′-RACE protocol (GIBCO BRL). The full-length protein is named Cep135 and its secondary structure was predicted using the programs of Lupas et al. (1991).

cDNA fragments encoding full-length Cep135 as well as truncated polypeptides were further subcloned into the multicloning site of the eukaryotic expression vector, pCMV-HA, which allows for expression of a recombinant protein that is tagged with hemagglutinin (HA) at the NH_2 terminus (Matuliene et al., 1999). The series of deletion constructs used in this study is listed in Fig. 5: #10 (amino acids 29–1145), #0 (amino acids 648–1145), and #1 (amino acids 922–1145) were directly isolated from original pBluescript (pBS) clones found in the λUni-Zap library. The clone Δ5 (amino acids 648–812) was obtained by digestion of pBS-#0 with BamHI and XbaI, and Δ1 (BamHI/ClaI fragment, amino acids 29–173), Δ2 (BamHI/NheI fragment, amino acids 29–326), Δ3 (BamHI/XbaI fragment, amino acids 29–812), Δ11 (ClaI/NheI, amino acids 174–326), Δ12 (NheI/BsrFI fragment, amino acids 327–687), Δ13 (XbaI/NcoI fragment, amino acids 813–953), and Δ14 (XbaI/XhoI fragment, amino acids 813–1145) were isolated from pBS-#10. To express Cep135 polypeptides fused with GFP, full-length, #0, and Δ3 inserts were subcloned into the multicloning site of pEFGP-C1 as described previously (Matuliene et al., 1999).

Cell culture and immunofluorescence staining

CHO cells were grown as monolayers in Ham's F-10 medium containing 10% FCS (HyClone) (Kuriyama et al., 1995). Mouse embryonic fibroblasts lacking p53 (Fukasawa et al., 1996; a gift from Drs. K. Fukasawa and G. Vande Woude, Frederic Cancer Center, Frederick, MD) were cultured in FCS-containing DME medium. Cultured *Xenopus* fibroblasts (XL177) were maintained in L-15 medium (GIBCO BRL) supplemented with 10% FCS at 22°C. Sea urchin gametes obtained from *Lytechinus pictus* were prepared according to the procedure described previously (Kuriyama, 1989).

Cells/eggs on coverslips were fixed with methanol at −20°C, and then were rehydrated with 0.05% Tween-20–containing PBS (PBS-Tw20). Samples were treated with a mixture of primary antibodies that contained (a) monoclonal mouse anti-HA (Berkeley Antibody Co.) and polyclonal rabbit anti-Cep135 antibodies derived from clone #0; (b) monoclonal anti–α-tubulin (Sigma-Aldrich) or β-tubulin (Amersham Pharmacia Biotech) antibodies and polyclonal Cep135 antibodies; or (c) monoclonal α- or β-tubulin and polyclonal HA antibodies (Santa Cruz Biotechnology, Inc.). For double staining with other centrosomal antibodies, we used the following combinations: (d) monoclonal HA and polyclonal γ-tubulin antibodies (Vassilev et al., 1995); (e) monoclonal HA and polyclonal anti-pericentrin antibodies (Covance); (f) mouse polyclonal anti-Cep135 and rabbit polyclonal anti-pericentrin antibodies; or (g) mouse polyclonal Cep135 and polyclonal γ-tubulin antibodies. After incubation at 37°C for 30 min, the samples were washed with PBS-Tw20 and further treated with a mixture of secondary antibodies (fluorescein-conjugated anti–mouse plus Texas red–conjugated anti–rabbit antibodies). Microscopic observation was made on either an Olympus BH-2 or a Nikon eclipse microscope with epifluorescence optics. Immunoblotting analysis was done as described previously (Kuriyama et al., 1995).

Transfections and RNAi

HA- or GFP-tagged Cep135 polypeptides were expressed in CHO cells using liposome/lipid-mediated DNA transfection (Matuliene et al., 1999). 0.6–2 μg/ml purified plasmid DNA was mixed with either Lipofectamine (Life Technologies) or Fugene (Boehringer) transfection reagents according to the manufacturer's protocol. After inducing for 12 to 24 h, cells were washed with PBS and fixed with cold methanol. To enrich a mitotic cell population, cells were partially synchronized by adding 2.5–5 mM thymidine 2 h after transfection. After incubating for 12–16 h, the drug was removed and cells were further cultured in fresh Ham's F-10 for 5 h. The cells were treated with 0.05–0.1 μg/ml nocodazole for 4–5 h, washed free of drug, and allowed to recover for 20–50 min before fixation (Kuriyama et al., 1995).

For the RNA interference assay, we synthesized 21-nucleotide siRNA duplexes, comprised of a 19 nucleotide duplex region corresponding to Cep135 in CHO cells (ACUAGCGACCUACCUGAGG; nucleotide positions 8–26) and dTdT overhangs at each 3′ terminus (Dharmacon Research). Purified oligonucleotides were diluted in distilled water and an aliquot (1.4 μg) was introduced into CHO cells cultured in a six-well plate via liposome-mediated transfection as above. For multiple transfections, cells were split 30–48 h after the first transfection (RNAi-I), and then subjected to a second (RNAi-II) and third (RNAi-III) treatment with siRNA. Mock transfections were performed in an identical manner, except that siRNA was omitted. Cep135 fluorescence intensity in the knockout cells was measured using the ImagePro software package as previously described (Matuliene et al., 1999). Transfected cells with abnormal microtubule distribution were counted after double staining with tubulin and Cep135 antibodies.

Electron microscopy

Cells expressing GFP-tagged Cep135 polypeptides were marked with a diamond scribe and further processed for thin section electron microscopy (Ryu et al., 2000). For immunoelectron microscopy, we used a protocol for preembedding immunogold staining (Kuriyama, 1989; Ryu et al., 2000). In brief, CHO cells in a culture chamber were fixed with 3% formaldehyde in PEM (100 mM Pipes at pH 6.8, 1 mM EGTA, 1 mM $MgCl_2$) for 10 min at room temperature. After extraction in PEM containing 0.5% Triton X-100 for 10 min, the sample was washed three times with PBS, 10 min each, and incubated for 60 min at 37°C in 10% BSA containing PBS-Tw20. The cells were incubated with polyclonal Cep135 antibodies (1:500 diluted)

for 2 h at 37°C, washed with PBS-Tw20, and then blocked with 1–3% normal goat serum in PBS-Tw20 for 30 min at 37°C. After incubation with 6-nm colloidal gold–conjugated goat anti–rabbit IgG (1:2 dilution with 3% normal goat serum in PBS-Tw20; Electron Microscopy Sciences) for 5 h at 37°C, the sample was washed overnight and further fixed with 2.5% glutaraldehyde in PEM for 60 min at room temperature. After postfixation with 1% OsO_4 for 60 min, the sample was dehydrated through an ethanol series and embedded in Epon-Araldite plastic. Thin sections were cut on a LKB Nova ultramicrotome and stained with uranyl acetate and lead citrate.

For immunolocalization of Cep135 at the spindle pole, mitotic spindles were isolated from CHO cells and sedimented at 3,000 *g* for 10 min in an IEC clinical centrifuge (Kuriyama et al., 1995). The pellet was resuspended in a small volume of isolation buffer (2.5 mM Pipes, pH 6.8, 0.25% Triton X-100, 20 μg/ml taxol), mounted on polylysine-coated glass coverslips, and fixed with 0.1–1% glutaraldehyde for 30 min at room temperature. After rinsing and thoroughly reducing with 1 mg/ml $NaBH_4$, the sample was blocked with 10% BSA and incubated with the diluted antibody as described above.

This work was supported by National Institutes of Health grant GM55735 to R. Kuriyama.

Submitted: 17 August 2001
Revised: 8 November 2001
Accepted: 21 November 2001

References

Andersen, S.S. 1999. Molecular characteristics of the centrosome. *Int. Rev. Cytol.* 187:51–109.

Atkinson, S.J., and M. Stewart. 1991. Expression in *Escherichia coli* of fragments of the coiled-coil rod domain of rabbit myosin: influence of different regions of the molecule on aggregation and paracrystal formation. *J. Cell Sci.* 99:823–836.

Bornens, M. 1977. Is the centriole bound to the nuclear membrane? *Nature.* 270: 80–82.

Buendia, B., C. Antony, F. Verde, M. Bornens, and E. Karsenti. 1990. A centrosomal antigen localized on intermediate filaments and mitotic spindle poles. *J. Cell Sci.* 97:259–271.

Dictenberg, J.B., W. Zimmerman, C.A. Sparks, A. Young, C. Vidair, Y. Zheng, W. Carrington, F.S. Fay, and S.J. Doxsey. 1998. Pericentrin and gamma-tubulin form a protein complex and are organized into a novel lattice at the centrosome. *J. Cell Biol.* 141:163–174.

Doxsey, S. 2001. Re-evaluating centrosome function. *Nat. Rev. Mol. Cell Biol.* 2:688–698.

Elbashir, S.M., J. Harborth, W. Lendeckel, A. Yalcin, K. Weber, and T. Tuschi. 2001. Duplexes of 21-nucleotide RNAs mediate RNA interference in cultured mammalian cells. *Nature.* 411:494–498.

Francis, S.E., and T.N. Davis. 2000. The spindle pole body of *Saccharomyces cerevisiae*: architecture and assembly of the core components. *Curr. Top. Dev. Biol.* 49:105–132.

Fry, A.M., T. Mayor, P. Meraldi, Y.-D. Stierhof, K. Tanaka, and E.A. Nigg. 1998. C-Nap1, a novel centrosomal coiled-coil protein and candidate substrate of the cell cycle–regulated protein kinase Nek2. *J. Cell Biol.* 141:1563–1574.

Fukasawa, K., T. Choi, R. Kuriyama, J. Rulong, and G.F. Vande Woude. 1996. Abnormal centrosome amplification in the absence of p53. *Science.* 271: 1744–1747.

Heitlinger, E., M. Peter, M. Haner, L. Lustig, U. Aebi, and E.A. Nigg. 1991. Expression of chicken lamin B_2 in *Escherichia coli*: characterization of its structure, assembly, and molecular interactions. *J. Cell Biol.* 113:485–495.

Hobohm, U., and C. Sander. 1995. A sequence property approach to search in protein database. *J. Mol. Biol.* 251:390–399.

Ishikawa, K., T. Nagase, M. Suyama, N. Miyajima, A. Tanaka, H. Kotani, N. Nomura, and O. Ohara. 1998. Prediction of the coding sequences of unidentified human genes. X. The complete sequences of 100 new cDNA clones from brain which code for large proteins in vitro. *DNA Res.* 5:169–176.

Kellogg, D.R., C.M. Field, and B.M. Alberts. 1989. Identification of microtubule-associated proteins in the centrosome, spindle, and kinetochore of the early *Drosophila* embryo. *J. Cell Biol.* 109:2977–2991.

Kilmartin, J.V., S.L. Dyos, D. Kershaw, and J.T. Finch. 1993. A spacer protein in the *Saccharomyces cerevisiae* spindle pole body whose transcript is cell cycle–regulated. *J. Cell Biol.* 123:1175–1184.

Kimble, M., and R. Kuriyama. 1992. Functional components of microtubule-organizing centers. *Int. Rev. Cytol.* 136:1–50.

Kuriyama, R. 1989. 225-kilodalton phosphoprotein associated with mitotic centrosomes in sea urchin eggs. *Cell Motil. Cytoskeleton.* 12:90–103.

Kuriyama, R., and G.G. Borisy. 1981. Centriole cycle in Chinese hamster ovary cells as determined by whole-mount electron microscopy. *J. Cell Biol.* 91: 814–821.

Kuriyama, R., and K. Ensrud. 1999. Obtaining antibodies to spindle components. *Meth. Cell Biol.* 61:233–244.

Kuriyama, R., M. Kofron, R. Essner, T. Kato, S. Dragas-Granoic, C.K. Omoto, and A. Khodjakov. 1995. Characterization of a minus-end–directed kinesin-like motor protein from cultured mammalian cells. *J. Cell Biol.* 129:1049–1059.

Kuriyama, R., T. Ohta, G. Peng, J. Vogel, and R. Kuriyama. 2001. Methods for identification of centrosome-associated proteins. *Meth. Cell Biol.* 67:125–140.

Lange, B.M.H., and K. Gull. 1995. A molecular marker for centriole maturation in the mammalian cell cycle. *J. Cell Biol.* 130:919–927.

Lupas, A., M. Van Dyke, and J. Stock. 1991. Predicting coiled coils from protein sequences. *Science.* 252:1162–1164.

Matuliene, J., R. Essner, J.-H. Ryu, Y. Hamaguchi, P.W. Baas, T. Haraguchi, Y. Hiraoka, and R. Kuriyama. 1999. Function of a minus-end-directed kinesin-like motor protein in mammalian cells. *J. Cell Sci.* 112:4041–4051.

Mazia, D. 1987. The chromosome cycle and the centrosome cycle in the mitotic cycle. *Int. Rev. Cytol.* 100:49–92.

Mogensen, M.M., A. Malik, M. Piel, V. Bouckson-Castaing, and M. Bornens. 2000. Microtubule minus-end anchorage at centrosomal and non-centrosomal site: the role of ninein. *J. Cell Sci.* 113:3013–3023.

Nakagawa, Y., Y. Yamane, T. Okanoue, S. Tsukita, and S. Tsukita. 2001. Outer dense fiber 2 is a widespread centrosome scaffold component preferentially associated with mother centrioles: its identification from isolated centrosomes. *Mol. Biol. Cell.* 12:1687–1697.

Nakamura, M., H. Masuda, J. Horii, K. Kuma, N. Yokoyama, T. Ohba, H. Nishitani, T. Miyata, M. Tanaka, and T. Nishimoto. 1998. When overexpressed, a novel centrosomal protein, RanBPM, causes ectopic microtubule nucleation similar to γ-tubulin. *J. Cell Biol.* 143:1041–1052.

Oegema, K., W.G.F. Whitefield, and B. Alberts. 1995. The cell cycle–dependent localization of the CP190 centrosomal protein is determined by the coordinate action of two separable domains. *J. Cell Biol.* 131:1261–1273.

Paoletti, A., M. Moudjou, M. Paintrand, J.L. Salisbury, and M. Bornens. 1996. Most of centrin in animal cells is not centrosome-associated and centrosomal centrin is confined to the distal lumen of centrioles. *J. Cell Sci.* 109:3089–3102.

Paul, E.C.A., and A. Quarani. 1993. Identification of a 102 kDa protein (cytocentrin) immunologically related to keratin 19, which is a cytoplasmically derived component of the mitotic spindle pole. *J. Cell Sci.* 106:967–981.

Ryu, J.-H., R. Essner, T. Ohta, and R. Kuriyama. 2000. Filamentous polymers induced by overexpression of a novel centrosomal protein, Cep135. *Microscopy Res. Tech.* 49:478–486.

Saredi, A., L. Howard, and D.A. Compton. 1996. NuMA assembles into an extensive filamentous structure when expressed in the cell cytoplasm. *J. Cell Sci.* 109:619–630.

Schatten, H., M. Walter, D. Mazia, H. Biessmann, N. Paweletz, G. Coffe, and G. Schatten. 1987. Centrosome detection in sea urchin eggs with a monoclonal antibody against *Drosophila* intermediate filament proteins: characterization of stages of the division cycle of centrosomes. *Proc. Natl. Acad. Sci. USA.* 84: 8488–8492.

Schmidt, P.H., D.T. Dransfield, J.O. Claudio, R.G. Hawley, K.W. Trotter, S.L. Milgram, and R. Goldenring. 1999. AKAP350, a multiply spliced protein kinase A-anchoring protein associated with centrosomes. *J. Biol. Chem.* 274: 3055–3066.

Schnackenberg, B.J., A. Khodjakov, C.L. Rieder, and R.E. Palazzo. 1998. The disassembly and reassembly of functional centrosomes in vitro. *Proc. Natl. Acad. Sci. USA.* 95:9295–9300.

Sellitto, C., M. Kimble, and R. Kuriyama. 1992. Heterogeneity of microtubule organizing center components as revealed by monoclonal antibodies to mammalian centrosomes and to nucleus associated bodies from *Dictyostelium*. *Cell Motil. Cytoskeleton.* 22:7–24.

Shu, H.B., and H.C. Joshi. 1995. γ-Tubulin can both nucleate microtubule assembly and self-assemble into novel tubular structures in mammalian cells. *J. Cell Biol.* 130:1137–1147.

Stearns, T., and M. Winey. 1997. The cell center at 100. *Cell.* 91:303–309.

Stewart, M., R.A. Quinlan, and R.D. Moir. 1989. Molecular interactions in paracrystals of a fragment corresponding to the α-helical coiled-coil rod portion of glial fibrillary acidic protein: evidence for an antiparallel packing of molecules and polymorphism related to intermediate filament structure. *J. Cell Biol.* 109:225–234.

Sym, M., and G.S. Roeder. 1995. Zip1-induced changes in synaptonemal complex structure and polycomplex assembly. *J. Cell Biol.* 128:455–466.

Tassin, A.M., C. Celati, M. Paintrand, and M. Bornens. 1998. Identification of an Spc110p-related protein in vertebrates. *J. Cell Sci.* 110:2533–2545.

Vassilev, A., M. Kimble, C.D. Silflow, M. LaVoie, and R. Kuriyama. 1995. Identification of intrinsic dimer and overexpressed monomeric forms of γ-tubulin in Sf9 cells infected with baculovirus containing the *Chlamydomonas* γ-tubulin sequence. *J. Cell Sci.* 108:1083–1092.

Vogel, J., T. Sterans, C. Rieder, and R. Palazzo. 1997. Centrosome isolated from *Spisula solidissima* oocytes contain rings and unusual stoichiometric ratio of α/β tubulin. *J. Cell Biol.* 137:193–202.

Wiese, C., and Y. Zheng. 1999. Gamma-tubulin complexes and their interaction with microtubule-organizing centers. *Curr. Opin. Struct. Biol.* 9:250–259.

Wigge, P.A., O.N. Jensen, S. Holmes, S. Soues, M. Mann, and J.V. Kilmartin. 1998. Analysis of the *Saccharomyces* spindle pole by matrix-assisted laser desorption/ionization (MALDI) mass spectrometry. *J. Cell Biol.* 141:967–977.

Xie, X., S. Rao, P. Walian, V. Hatch, G.N. Phillips, Jr., and C. Cohen. 1994. Coiled-coil packing in spermine-induced tropomyosin crystals. A comparative study of three forms. *J. Mol. Biol.* 236:1212–1226.

Zhou, H., J. Kuang, L. Zhong, W.L. Kuo, J.W. Gray, A. Sahin, B.R. Brinkley, and S. Sen. 1998. Tumour amplified kinase STK15/BTAK induces centrosome amplification, aneuploidy and transformation. *Nat. Genet.* 20:189–193.